ADVANCES IN FOREST FIRE RESEARCH

2022

Edited by
DOMINGOS XAVIER VIEGAS
LUÍS MÁRIO RIBEIRO

Generic burning rate curve for porous fuel beds

Sara McAllister*; Isaac Grenfell; Mark Finney

RMRS Missoula Fire Sciences Lab, USDA Forest Service. 5775 W US Highway 10, Missoula, MT 59808, USA, {sara.mcallister; isaac.c.grenfell; mark.finney}@usda.gov

**Corresponding author*

Keywords

Burning rate, wood cribs, design fire

Abstract

A new wildfire spread model is being developed to alleviate many of the limitations of current operational models. This new model consists of sub-models for ignition, burning and heat release rate, and heat transfer. Unfortunately, the factors that control the burning rate of wildland fuels are not well understood. In this work, we use an extensive database of experimental data with wood cribs to examine curve forms that can be used to describe the time-dependent nature of the burning rate of porous fuel beds. Fifty crib designs and 148 individual mass data curves of cribs burned with unrestricted airflow were available for analysis. Both a power law and a Weibull-distribution-like curve are shown to capture the main shape of the experimental data. Further work will incorporate data with restricted airflow, wind, and moisture content.

1. Introduction

Operational fire behaviour models are either empirically (such as the Canadian and Australian systems (Fire Danger Group 1992, Cruz et al. 2015)) or semi-empirically derived (Rothermel model in the US system (Rothermel 1972). Because of their origin, there are inherent limitations to their use. For example, these three systems consist of fire spread models, designed to output a spread rate for a given set of conditions. There is no built-in ability to determine if a fire will even spread, a question that is relevant to planning prescribed fires and determining the burning period for long duration modelling. In order to alleviate such limitations, a new fire behaviour model is being developed by the Missoula Fire Sciences Lab that treats fire spread as a series of ignitions (Finney et al. 2021). Once an initial ignition is realized, the fuel begins to burn releasing heat at a given rate, and some of that heat is transferred to the unburnt fuel ahead. The new fire behaviour model thus consists of several sub-models: ignition, burning and heat release rate, and heat transfer. This paper focuses on work towards the burning and heat release rate sub-model.

Unfortunately, the burning rates of wildland fuels beds are not well understood. Though it is not actually used in spread prediction, the related residence time of a wildland fire is predicted in BehavePlus as simply 8 times the fuel diameter in inches, which does not take into consideration the variety of other parameters that are likely at play, such as packing, moisture content, and wind (Albini 1976, Anderson 1969). Studying the burning rate in natural fuels beds during a spreading fire is very challenging and it is difficult to accurately manipulate the relevant variables to understand the underlying governing physical processes. For this reason, a simplified fuel bed is often used called a wood crib. Wood cribs have been used to study wildland fire for decades (Fons 1963, Byram 1964, Rothermel 1971, Thomas 1973, Anderson 1990). Wood cribs are frequently used in fire protection engineering as ignition sources and there are several correlations to predict their burning rates (Gross 1962, Block 1971, Heskestad 1973, Thomas 1973). Previous work (McAllister and Finney 2016a) has shown that a slightly modified version (from McAllister and Finney 2016a) of the correlation from Thomas (1973) works best to predict the burning rate for a wide variety of crib designs and stick thicknesses:

$$\frac{100\dot{m}}{A_s\rho_o(gh)^{0.5}} = \frac{0.85}{(0.26h/s)} \qquad \text{(Eq. 1)}$$

where $\dot{m}$ is the burning rate (g/s), A_s is the exposed surface area (cm^2), ρ_o is the air density (g/cm^3), h is the crib height (cm), and s is the spacing between sticks (cm). The new fire behaviour model under development currently uses a simple empirical relation based on a somewhat limited set of laboratory experiments as a place

holder for a more complete sub-model. This place holder consists of a burning rate that is constant in time, which is a gross simplification for the time-dependent burning rate so often seen in actual scenarios where the fire builds in intensity, reaches a peak, and then decays to extinction. The goal of this paper is to develop a more physically-based time-dependent relation for the burning rate based on experiments using wood cribs. Such a "design fire" is common in the fire protection literature (for example see Bwalya 2008, Quintiere 2017).

2. Methods

McAllister et al. have conducted a wide range of experiments using wood cribs and have generated an extensive database of experimental data that will be exploited for this work (see McAllister and Finney 2016a, McAllister and Finney 2016b, McAllister 2019, McAllister 2021, McAllister 2022). For a detailed description of the experimental procedures, please see the original papers. The same general procedure was followed. The cribs were conditioned in a conditioning chamber at 35°C and 3% RH for at least three days so that the moisture content was about 1%. The cribs were place on 7.62 cm tall rectangular steel tubes to create a sufficient space between the crib and the weighing platform (see McAllister and Finney 2016a). The cribs were ignited by briefly dunking them in 99% isopropyl alcohol and allowing them to drain. The mass was measured with three 6-kg load cells recording at 10 Hz for the majority of tests. The reported burning rates were found by determining the maximum slope of a linear fit to the data. In all, the database consists of 50 crib designs with a wide variety of stick thickness (0.16-1.27 cm), stick lengths (6.4-60.96 cm), crib heights (1.27-31.75 cm), and porosities (0.00196-0.211 as evaluated by the Heskestad (1973) formulation). See Appendix A for a full list of crib designs. Most cribs were tested three times so a total of 148 mass loss curves were available for analysis.

To prepare the data for analysis, the data was trimmed to only include the time when the crib was actively burning. The ignition point was manually determined, but the burnout time was chosen to be the time when the burning rate, found from a spline fit with ten degrees of freedom, dropped to 5% of the peak value. The consumed mass (initial mass – mass(t)) was then scaled by the initial mass minus the residual mass, and the time scaled by the burnout time so that both mass and time ranged between 0 and 1. The scaled burning rate was found by a spline fit of the scaled mass and scaled time. The scaling can be done for both the consumed mass and burning rate with the measured values ("observed scaling") as well as predicted values ("predicted scaling") based on the number of sticks, wood density, and peak burning rate estimated from the Thomas correlation (Equation 1). Because the peak burning rate only occurs in most cases for a short period of time, an average burning rate would be more appropriate to estimate the burnout time. To estimate this average burning rate as a proportion of the peak, a subset of the data was examined, and it was found that the average burning rate was approximately 60% of the peak value. Thus, an average scaled burning rate of 0.60*(peak burning rate) was used to estimate the predicted burnout time for scaling the data (predicted burnout time = predicted initial mass / average predicted burning rate). Two curve forms were then fit to this collection of scaled data, first with the scaled consumed mass then the scaled burning rate. The first curve form, a power-law relation, was used based on experience:

$$m^*_{consumed} = \left(\frac{2t^*}{1+t^{*\alpha}}\right)^{\beta} \qquad \text{(Eq. 2)}$$

The second was found from a literature survey to be quite useful for fitting heat release rate curves from cone calorimeter tests to passenger vehicles (Numajiri and Furukawa 1998, Ingason 2005, Tohir et al. 2021):

$$m^*_{consumed} = \left[1 - e^{-\gamma t^*}\right]^{\delta} \qquad \text{(Eq. 3)}$$

where $m^*_{consumed}$ is the scaled consumed mass (dimensionless), t* is the scaled time (dimensionless), and α, β, γ, and δ are fitting constants. Note that Equation 3 is similar to the Weibull distribution but will be referred to here as the "N&F" fit in reference to the work by Numajiri and Furukawa (1998). The derivatives of Eqs. 2 and 3 were used to fit the scaled burning rate:

$$\dot{m}^* = 2\beta\left(\frac{2t^*}{1+t^{*\alpha}}\right)^{\beta-1}\frac{1+(1-\alpha)t^{*\alpha}}{(1+t^{*\alpha})^2} \qquad \text{(Eq. 4)}$$

$$\dot{m}^* = \gamma\delta e^{-\gamma t^*}\left[1 - e^{-\gamma t^*}\right]^{\delta-1} \qquad \text{(Eq. 5)}$$

where $\dot{m}^*$ is the scaled burning rate (dimensionless).

3. Results and Discussion

Table 1 shows the fitting constants in Equations 2 and 3 that best fit the experimental scaled consumed mass ("mass curve fits") and the fitting constants in Equations 4 and 5 for the scaled burning rate ("rate curve fits"). Also included in Table 1 are measures of fit including the coefficient of determination (r^2), root-mean-square error/deviation (RMSE), and the median absolute error/deviation (MDAE).

Table 1 – Curve fit constants and measures of fit for "observed scaling."

	Power law mass curve fit (Eq. 2)	N&F mass curve fit (Eq. 3)	Power law rate curve fit (Eq. 4)	N&F rate curve fit (Eq. 5)
Fitting constant 1 [ ]	$\alpha = 1.450$	$\gamma = 3.784$	$\alpha = 1.687$	$\gamma = 3.212$
Fitting constant 2 [ ]	$\beta = 1.845$	$\delta = 3.265$	$\beta = 2.160$	$\delta = 3.250$
r^2 to mass [ ]	0.9593	0.9535	0.9620	0.9614
RMSE to mass [ ]	0.0659	0.0713	0.0688	0.1044
MDAE to mass [ ]	0.0407	0.0519	0.0448	0.0846
r^2 to rate [ ]	0.5206	0.4879	0.6006	0.5470
RMSE to rate [ ]	0.3281	0.3735	0.3093	0.3203
MDAE to rate [ ]	0.2652	0.2690	0.2329	0.2418

Figure 1 compares the "mass curve fits" to the experimental mass consumed data using both the "observed scaling" on the left and the "predicted scaling" on the right. Immediately, it is observed that there is considerably more spread in the data when the "predicted scaling" is used. This is due to the accumulation of errors in estimating the initial mass (7.7% average difference from observed), the residual mass (29-31% for 1.27 and 0.64 cm sticks; 110-117% for 0.32 and 0.16 cm sticks), and the burning time (30% average difference from observed). A noticeable portion of the spread is from a handful of crib designs whose burning rate (and thus burning time) was not well predicted by the Thomas correlation (Eq. 1). In general, however, both curve fits are centred in the data cloud, with the power law (red) curve appearing to increase at a slightly earlier time than the N&F (blue) curve and pass through the point (1, 1).

Figure 2 compares the "mass curve fits" to the scaled burning rates using both the "observed scaling" on the left and the "predicted scaling" on the right. Here again, as expected, when the "predicted scaling" is used there is more spread in the data for the same reasons as above. What is more problematic is that the time when the peak burning rate occurs does not seem to be well predicted when the consumed mass is used for fitting. Key metrics for the burning rate are compared in Table 2. The "experimental" values are averages from each individual data file. By considering the first three columns in Table 2, it appears that power law fit to the consumed mass data might be slightly better at matching the time to the peak scaled burning rate, but the N&F curve fit to the consumed mass data is better for capturing the mean and peak scaled burning rates.

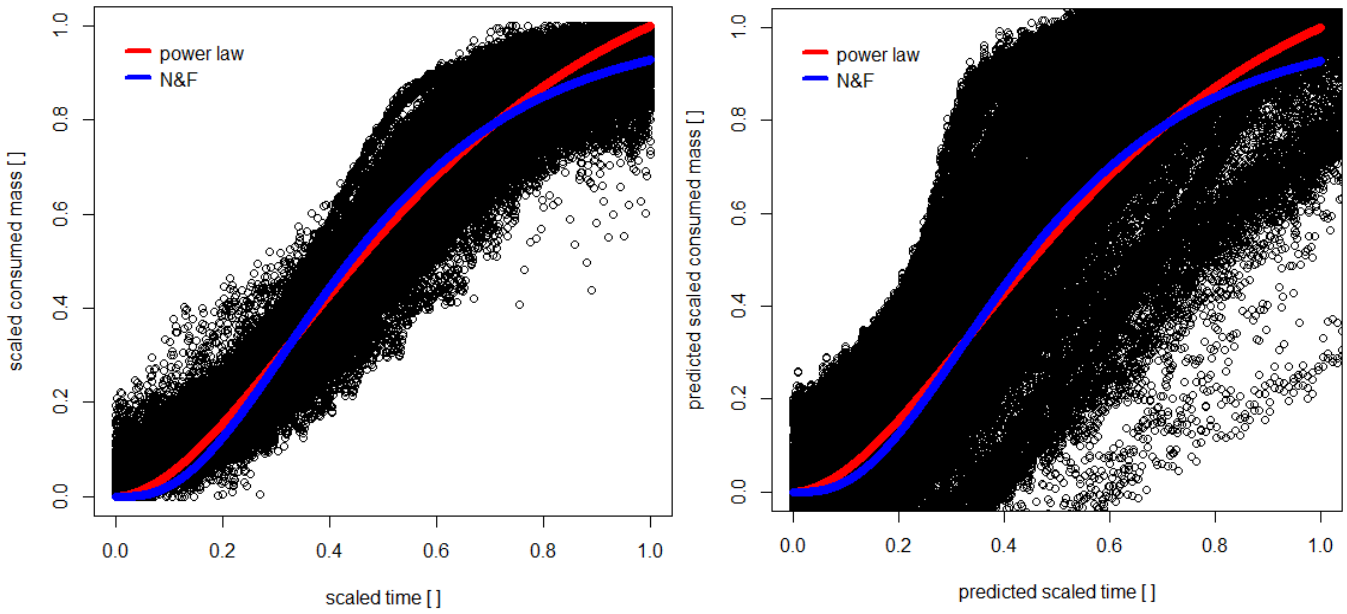

Figure 1 – "Mass curve fits" for consumed mass versus time using observed scaling (left) and predicted scaling (right).

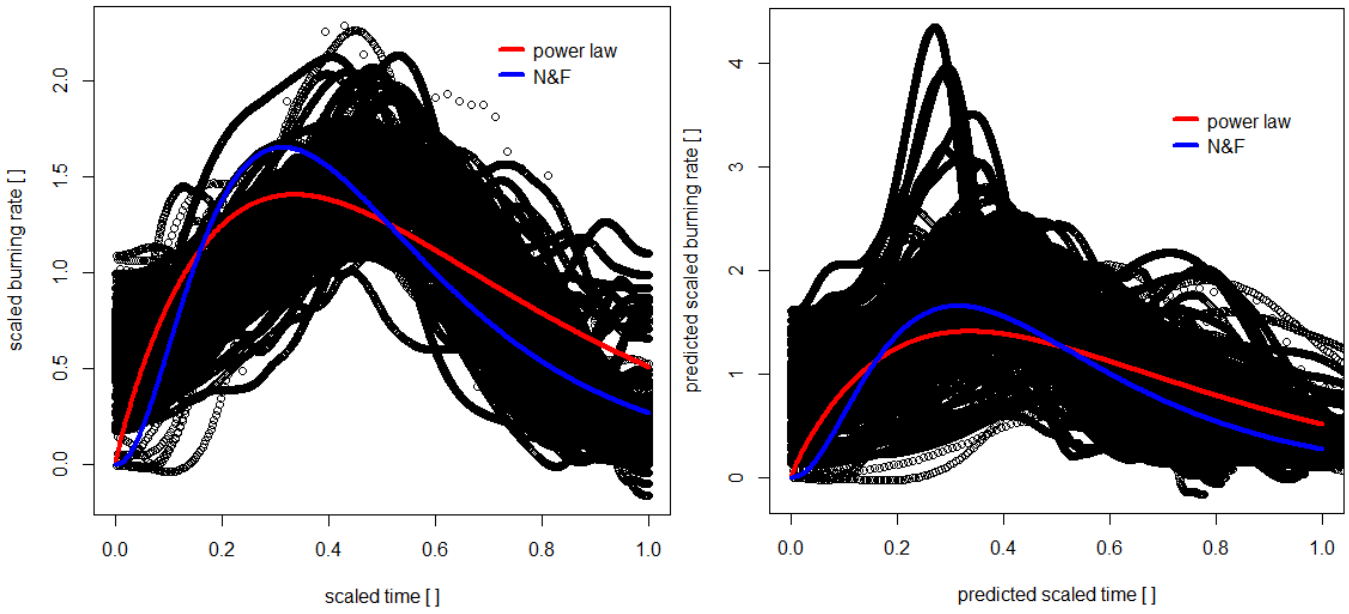

Figure 2 – "Mass curve fits" applied to scaled burning rate using observed scaling (left) and predicted scaling (right).

Table 2 – Key burning rate parameters as measured in the database and calculated from curve fits.

Burning rate parameter	Experimental average	Power law to mass data (Eq. 2)	N&F to mass data (Eq. 3)	Power law to rate data (Eq. 4)	N&F to rate data (Eq. 5)
Mean scaled burning rate [ ]	0.9286	1.000	0.9276	0.9992	0.8742
Peak scaled burning rate [ ]	1.5940	1.4057	1.6527	1.5477	1.4041
Time to peak scaled rate [ ]	0.4949	0.333	0.312	0.386	0.367

Figure 3 shows the results if the curves in Eqs. 4 and 5 are fit to the scaled burning rate (using the "observed scaling"). As shown in Table 1, the curve fitting constants and goodness of fits are slightly different. As expected, the measures of fit to the rate data have improved, while the fitness has decreased slightly for the consumed mass. Though the differences between the two curve fits are still slight, Table 2 shows that when the burning rate is fit, the time to peak is shifted somewhat to match the experimental average more closely but is

still skewed slightly early. The power law fit now slightly better predicts the peak burning rate, while the N&F still better matches the average.

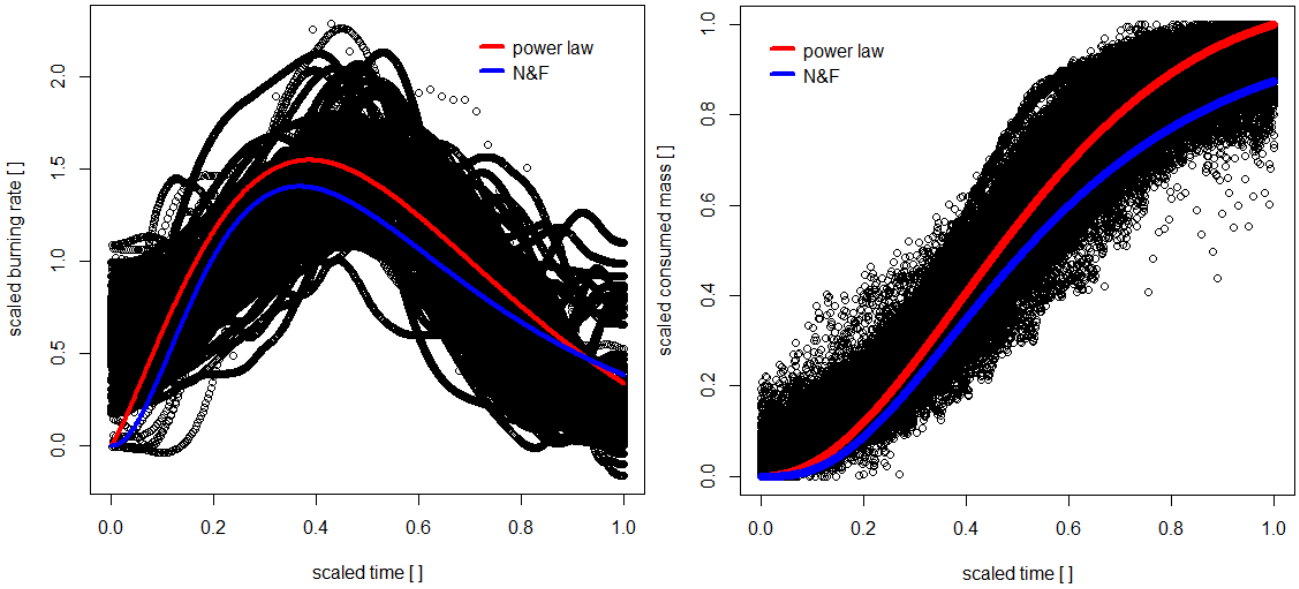

Figure 3 – "Rate curve fits" plotted with scaled burning rate data (left) and scaled consumed mass (right).

4. Summary and Future Work

Two curve forms were fit to an experimental database of crib burns. Both curve forms show promise and captures features of the data slightly differently. Determination of which curve form is most appropriate will likely depend on which feature is more important to the application. Further data also needs to be incorporated that includes the effect of restricted air flow, wind, and moisture content.

5. Acknowledgements

This work was funded by the National Fire Decision Support Centre. The authors want to thank James McGuire, Jennifer Kennedy, Sophia Vernholm, and Chelsea Phillips for building the many cribs and help performing the experiments; Randy Pryhorocki and Josh Deering for building the apparatuses used for the experiments; and Cyle Wold for setting up the data acquisition system.

6. References

F.A. Albini. 1976. Estimating wildfire behavior and effects. General Technical Report INT-30, Intermountain Research Station, USDA Forest Service. (Ogden, UT)

H.E. Anderson. 1969. Heat transfer and fire spread. Research Paper INT-69, Intermountain Research Station, USDA Forest Service. (Ogden, UT)

H.E. Anderson. 1990. Relationship of fuel size and spacing to combustion characteristics of laboratory fuel cribs,'' Research Paper INT-424, Intermountain Research Station, USDA Forest Service.

G.M. Byram, H.B. Clements, E.R. Elliott, P.M. George. 1964. An experimental study of model fires, Technical Report No. 3, Forest Service, USDA Southeastern Forest Experiment Station.

A. Bwalya. 2008. An Overview of Design Fires for Building Compartments. *Fire Technol* **44,** 167–184.

M.G. Cruz, J.S. Gould, M.E. Alexander, A.L. Sullivan, W.L. McCaw, S. Matthews. 2015. A guide to the rate of fire spread models for Australian vegetation. Australasian Fire and Emergency Service Authorities Council Ltd. And Commonwealth Scientific and Industrial Research Organisation, Melbourne, Vic, 123 pp.

M.A. Finney, S.S. McAllister, T.P. Grumstrup, J.M. Forthofer. 2021. Wildland fire behavior: dynamics, principles and processes, CSIRO Publishing, Clayton South, Victoria, Australia, 360 pp.

Fire Danger Group. 1992. Development and Structure of the Canadian Forest Fire Behavior Prediction System. Vol. 3. Forestry Canada, Science and Sustainable Development Directorate.
G. Heskestad. 1973. Modeling of enclosure fires, *Symp. (Int.) Combust.* 14, 1021-1030.
H. Ingason. 2005. Fire development in large tunnel fires, Fire Saf. Sci. 8, 1497–1508,
S. McAllister, M. Finney. 2016a. Burning rates of wood cribs with implications for wildland fires. *Fire Technol* 52, 1755-1777.
S. McAllister, M. Finney. 2016b. The effect of wind of burning rate of wood cribs, Fire Technol 52, 1035-1050.
S. McAllister. 2019. The Role of Fuel Bed Geometry and Wind on the Burning Rate of Porous Fuels, *Front. Mech. Eng.* 5, 11. doi: 10.3389/fmech.2019.00011
S. McAllister. 2021. Effect of reduced plume entrainment on the burning rate of porous fuel beds. Progress in Scale Modeling, an International Journal 2(2), 6. doi: 10.13023/psmij.2021.02-02-06
S. McAllister. 2022. Burning rate and flow resistance through porous fuel beds: axisymmetric versus line fires, *Combust Sci Technol* DOI: 10.1080/00102202.2021.2019233
J.G. Quintiere. 2017. Principles of Fire Behavior, 2nd edition, CRC Press, New York, 413 pp.
R.C. Rothermel. 1972. A mathematical model for predicting fire spread in wildland fuels. Research Paper INT-115, Intermountain Research Station, USDA Forest Service, 40 pp.
P.H. Thomas. 1973. Behavior of fires in enclosures – some recent progress, *Symp. (Int.) Combust*. 14, 1007-1020.
M.Z.M. Tohir, M. Spearpoint, C. Fleischmann. 2021. Probabalistic design fires for passenger vehicle scenarios, Fire Safety Journal 120, 103039. Doi: https://doi.org/10.1016/j.firesaf.2020.103039

Table A.1 – Crib designs in database. The crib porosity is calculated using the method from Heskestad (1973). Cribs with a porosity less than 0.05 cm are considered densely packed.

crib design no	stick thickness (b, [cm])	height (h, [cm])	No sticks per layer (n, [])	No. layers (N, [])	stick length (l, cm)	packing ratio	Heskestad porosity (cm)
1	1.27	31.75	2	25	12.7	0.20	0.1205
2	1.27	12.7	3	10	12.7	0.30	0.1060
3	1.27	17.78	3	14	15.24	0.25	0.1169
4	1.27	12.7	5	10	12.7	0.50	0.0215
5	1.27	12.7	7	10	12.7	0.70	0.0039
6	1.27	17.78	6	14	20.3	0.38	0.0390
7	1.27	26.67	4	21	25.4	0.20	0.1202
8	1.27	2.54	11	2	25.4	0.55	0.0625
9	1.27	6.35	10	5	30.48	0.42	0.0757
10	1.27	3.81	13	3	40.64	0.41	0.1313
11	1.27	3.81	14	3	43.18	0.41	0.1257
12	1.27	5.08	13	4	45.72	0.36	0.1414
13	0.64	6.35	3	10	6.4	0.30	0.0530
14	0.64	6.35	5	10	6.4	0.50	0.0108
15	0.64	6.35	7	10	6.4	0.71	0.0020
16	0.64	15.24	6	24	12.7	0.30	0.0205
17	0.64	8.89	4	14	15.24	0.17	0.1293
18	0.64	5.715	5	9	15.24	0.21	0.1246
19	0.64	22.23	10	35	15.24	0.42	0.0057
20	0.64	8.89	8	14	19.05	0.27	0.0454
21	0.64	9.53	5	15	19.05	0.17	0.1174

22	0.64	10.16	8	16	19.69	0.26	0.0429
23	0.64	28.58	3	45	20.32	0.10	0.1213
24	0.64	10.16	8	16	20.32	0.25	0.0460
25	0.64	10.16	10	16	20.32	0.32	0.0270
26	0.64	8.89	9	14	20.96	0.28	0.0429
27	0.64	9.53	9	15	21.59	0.27	0.0429
28	0.64	5.08	8	8	22.86	0.23	0.1179
29	0.64	6.35	6	10	25.4	0.15	0.211
30	0.64	3.81	10	6	25.4	0.25	0.1197
31	0.64	6.35	10	10	25.4	0.25	0.0725
32	0.64	9.53	14	15	25.4	0.36	0.0213
33	0.64	1.91	27	3	25.4	0.69	0.0074
34	0.64	8.89	8	14	30.48	0.17	0.1210
35	0.64	3.81	12	6	30.48	0.25	0.1188
36	0.64	4.45	20	7	30.48	0.42	0.0270
37	0.64	5.72	20	9	60.96	0.21	0.1163
38	0.32	3.81	6	12	15.24	0.13	0.1232
39	0.32	3.81	8	12	20.32	0.13	0.1206
40	0.32	1.27	14	4	20.32	0.22	0.1173
41	0.32	1.91	14	6	25.4	0.18	0.1242
42	0.32	9.54	14	30	25.4	0.18	0.0252
43	0.32	6.36	27	20	25.4	0.34	0.0087
44	0.32	12.72	6	40	30.48	0.06	0.1215
45	0.32	2.86	14	9	30.48	0.15	0.1178
46	0.16	1.59	9	10	15.24	0.10	0.1191
47	0.16	11.11	3	70	15.24	0.03	0.1173
48	0.16	1.27	13	8	20.32	0.10	0.1272
49	0.16	5.72	15	36	20.32	0.12	0.0220
50	0.16	1.27	16	8	25.4	0.10	0.1298